

**ICF1001026OR**

**DETERMINATION OF MICROSTRUCTURAL  
PARAMETERS FOR MODELING OF FATIGUE  
BEHAVIOR OF CERAMICS**

M. Boudrare<sup>1</sup>, R. D. Geraghty<sup>2</sup>, C. Ortiz<sup>3</sup> and Kenneth W. White<sup>4</sup>

<sup>1,4</sup>Department of Mechanical Engineering, University of Houston,  
Houston, TX, 77204-4792, U.S.A.

<sup>2</sup>Calpine Corp., Houston, TX

<sup>3</sup>Johnson Space Center, NASA Houston, TX

**ABSTRACT**

This study examines the microstructural role of crack face bridging mechanisms in a monolithic ceramic, subjected to cyclic loading conditions at room and high temperatures. By utilizing a unique post-fracture-tensile experiment, the fatigue properties of a commercially available alumina are examined. Based on the current results, one will conclude that the wake zone bridging consists of a combination of bridging by frictional and unbroken ligaments. At room temperature, when the peak loads, initial crack opening displacement and number of cycles are held below values which cause grain sliding, no fatigue damage is evident. Above the threshold values, however, notable damage may be observed. This cumulative wear process reduces the effectiveness of the bridging. At high temperature, it was found that the relaxation of normal forces due to the softening of the grain boundary phase gives a rise to ratcheting behavior. For the quasistatic bridging problem, accumulation of damage has been related to grain size features, but apparent from data in this study, fatigue related damage depends upon damage to sub-grain size features.

**KEYWORDS**

Ceramics, Toughness, Bridging mechanism, Fatigue, Thermal expansion Anisotropy.

## INTRODUCTION

In the past, ceramics were considered to be immune to fatigue damage from cyclic loading due to their low dislocation mobility and corresponding lack of crack-tip plasticity [1]. Despite several early observations to the contrary [2,3], enhanced crack propagation under cyclic loading was commonly attributed to environmentally induced stress corrosion cracking [4]. However, recent work has demonstrated a true fatigue effect in many ceramics, such as  $\text{Al}_2\text{O}_3$  [5-13] and  $\text{Si}_3\text{N}_4$  [10,13-17], where subcritical crack growth rates, under cyclic loads, can greatly exceed growth rates under static loads at equivalent stress intensity levels. As a part of this new interest the question arises - what role does the microstructure play in the behavior, and specifically, how do the bridging grains contribute to fatigue crack growth resistance?

It is now well recognized that the toughness of many non-transforming monolithic ceramics, under monotonic loading often increases as the crack extends, resulting in a rising crack growth resistance (R) curve [18]. This toughening behavior is primarily due to grain bridging in the wake zone of the advancing crack, which reduces the effective stress intensity factor at the crack tip [19-21].

During cyclic loading, it has been suggested that the degradation of such toughening mechanisms promotes fatigue crack growth. Indeed, recent work [9-12,17,23] has indicated that in grain bridging ceramics, repetitive sliding wear of the bridging grains, under cyclic loading, reduces the load bearing capacity of these wake zone elements and lowers the toughness of the material. Lathabai, *et al* [23], modeled the decreased bridging capacity under cyclic loading by assuming a reduction in the frictional coefficient between the bridging grains and their sockets in the surrounding material. Also, a frictional wear mechanism was proposed by Dauskardt [10] in which a micromechanical model was developed to relate the reduction in grain pullout stresses to material removed by wear processes at the grain/socket interface. Indirect evidence for this mechanism of fatigue crack growth has also come from examination of fracture surfaces where wear tracts and wear debris have been observed [11,17,23].

The purpose of the present study is to examine the cyclic loading behavior in room and high temperature conditions of a monolithic alumina, which shows significant R-curve toughening by grain bridging. By utilizing an experiment called the post-fracture-tensile (PFT) test, developed by Hay and White [24-27], we are able to isolate discrete elements of the crack wake zone for detailed study. Previously, the PFT experiment has proven effective for the evaluation of the wake process zone resulting from quasistatic crack extension [24,26,27]. Of particular interest here is the damage induced by repeated loading and unloading of the bridging grains.

## PROCEDURES

### *Material and Specimens*

The alumina used in this study is a commercial 99.7% alumina, obtained through Johnson Matthey, and is the same as that characterized previously [24,27,30]. The average grain size, found from a polished and etched surface, is approximately 18  $\mu\text{m}$  and a majority of the grains (~90%) are less than 35  $\mu\text{m}$ . A monotonically loaded fracture surface, shown

in Figure 1 (a), indicates the size, morphology and spatial arrangement of the grains. The grain size distribution for this alumina, obtained from polished and etched surfaces, is shown in Figure 1 (b).

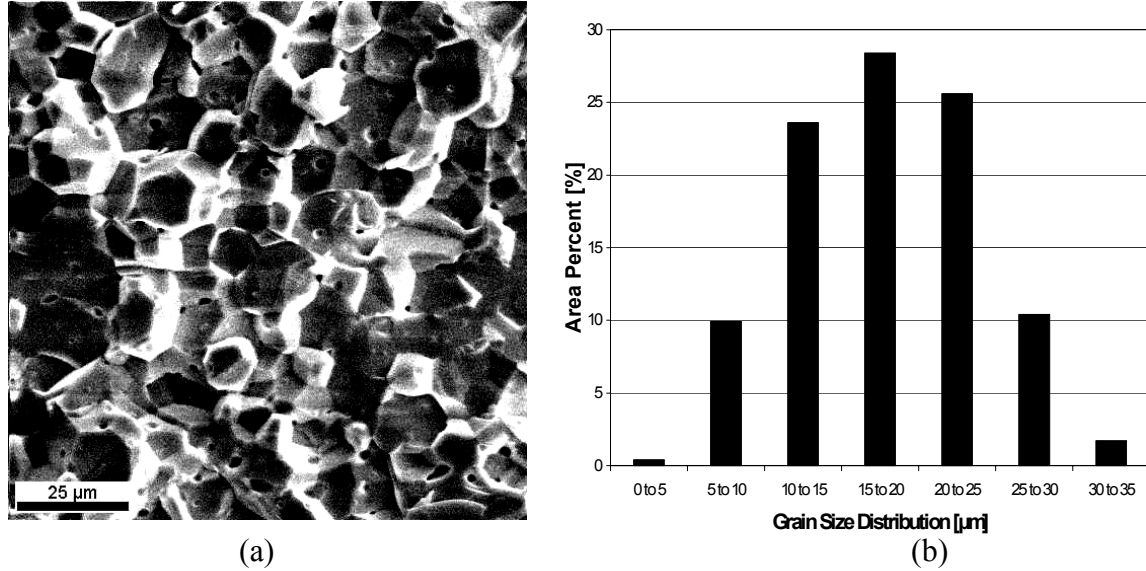


Figure 1: Fracture surface (a) and grain size distribution (b) of material studied

### *PFT Experiment*

To obtain R-curve information, and to provide specimens for the second stage of testing, double cantilever beam (DCB) specimens were cut from bulk plates measuring 50 mm x 100 mm x 4 mm. A schematic of the specimen is shown in Fig. 2(a), where  $h=8.5\text{mm}$ ,  $w=4\text{mm}$ ,  $w'=2\text{mm}$ ,  $L=48\text{mm}$ , and  $a_0=13\text{mm}$ . A half-thickness side groove down the center of the specimen restricts crack deviation from the desired fracture plane. Specimens were fractured on an Instron testing machine at a displacement rate of  $0.75\ \mu\text{m}/\text{min}$ . Crack lengths were observed optically and crack growth was arrested by load removal when the crack had grown approximately 16 mm. Figure 2(b) shows the R-curve data obtained for this microstructure, where a plateau  $K_R$  value of  $4.6\text{MPa}\cdot\text{m}^{1/2}$  is reached after 9mm of crack extension.

The second part of the experiment, referred to as the post-fracture tensile (PFT) test, requires the machining of tensile specimens from the cracked DCB specimen for the direct characterization of the bridging mechanism. The PFT technique provides a unique tool to isolate incremental segments of the crack-wake. Shown in Figure 2(a), the region behind the crack tip is sliced into several 1mm wide strips. Each strip is through-cracked and held together only by bridging elements as shown by the schematic in Figure 3b. The two side grooves, which were machined prior to slicing, facilitate tensile loading on two knife-edges. We have examined the effects of introducing these PFT loading grooves prior to, or following the fracture test. Since the PFT data obtained by both methods are indistinguishable, we conclude the grooving step does not adversely affect the wake.

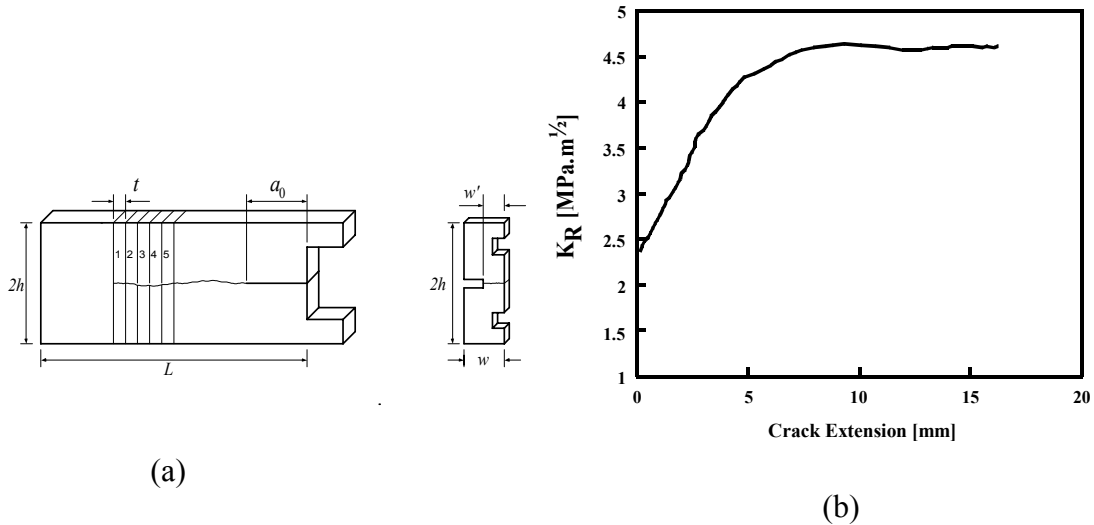


Figure 2: Schematic of DCB and PFT specimens (a), R-curve behavior of the alumina tested (b).

Details of the experimental setup and data collection techniques will not be elaborated upon here as they have been extensively outlined in previous publications [24-27]. For these particular results, three PFT specimens have been fatigued to obtain information on load-cycling effects at room temperature and high temperature. Two came from the position nearest the crack tip, which we call PFT#1 and PFT#2 (refer to Figure 2a) and the other came from the fifth position away from the tip, which we call PFT#5. All PFT specimens were subjected to series of cyclic tests.

## RESULTS AND DISCUSSION

In Figure 3(a), load-displacement data for the #1 PFT specimen is presented for two maximum loading conditions. From this data, it is evident that this specimen exhibits the same linear elastic type behavior at maximum load of 0.32 Kg before (Test1) and after (Test 2) 10,000 cycles, and the compliance remains constant at approximately 0.11  $\mu\text{m}/\text{kg}$ . Immediately following this test, PFT#1 was sinusoidally loaded to a higher maximum load of 0.72 kg and unloaded (Test 3), as shown in Figure 3(a). During this test we observe an interesting behavior evidenced by the formation of a hysteresis loop. Starting from the premise that the existence of this loop indicates the presence of some type of energy loss mechanism, we further assert that a damage mechanism, related to the fracture of the elastic ligaments and the sliding of the bridging grain, have been activated when the applied load or displacement reaches some critical value. Similar hysteretic behavior has been observed by Vekinis, *et al* [22] Dauskardt [10] in alumina and by Gilbert, *et al* [17] in silicon nitride.

The effects of cycling an additional 10,000 times to the same maximum load, 0.72 kg, are presented in Figure 3(b). From this data, two interesting points of note become

evident. Firstly, the initial elastic compliance remains unchanged at  $0.11 \mu\text{m}/\text{kg}$ . However, the load at which the behavior becomes non-linear has been reduced from  $0.41 \text{ kg}$  to  $0.32 \text{ kg}$ . This indicates that cycling the specimen a further 10,000 times at  $0.72 \text{ Kg}$  has reduced the effectiveness of the elastic bridging (Test 4). Secondly, as we approach the maximum load of the cycle, we observe a greater increase in the specimen compliance. In first cycle, this compliance reached  $0.22 \mu\text{m}/\text{kg}$ . However, after 10,000 cycles, it has increased quite substantially to  $0.63 \mu\text{m}/\text{kg}$  (refer to Test 4). These results indicate that a damage mechanism may have been activated due to the combination of fracture of elastic ligaments observed under the SEM and continuous sliding of the bridging grains. Those mechanisms, therefore, have the effect of degrading the bridging capacity and hence the toughening ability of this alumina has been reduced.

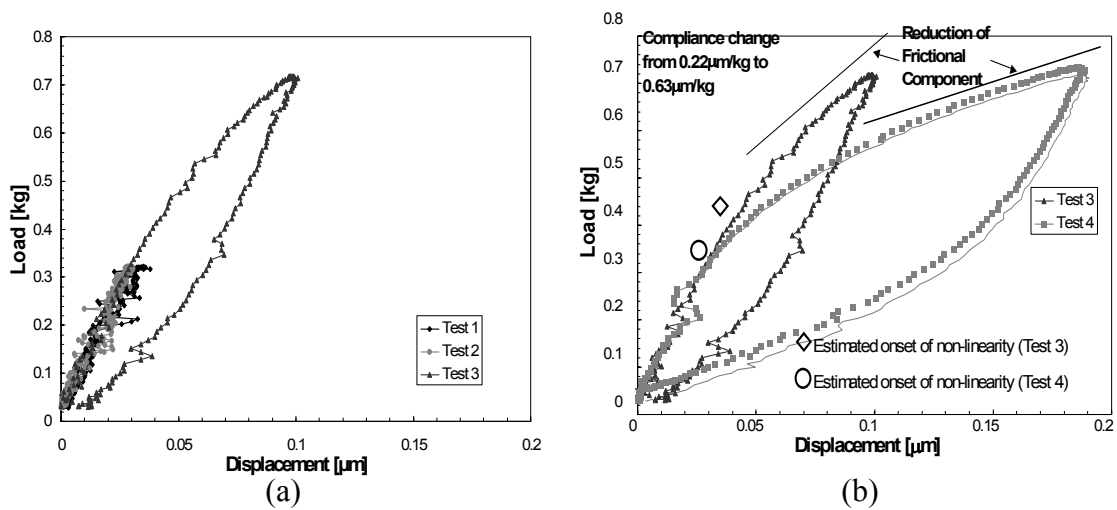


Figure 3: Load increase effect (a) and high cyclic loading effect (b)

The PFT procedure was used to investigate temperature effects on the wake zone behavior of alumina. Here, an isolated wake zone element obtained from a DCB was subjected to load cycling at various temperatures. A temperature interrupted PFT test was adapted to elucidate the effects of Thermal Expansion Anisotropy (TEA). The test consisted of initially testing a PFT at room temperature to obtain the load-displacement behavior. Continuation of the procedure then evaluated load-displacement behavior at  $600$  and  $800 \text{ }^\circ\text{C}$ , follow by a repetition of the room temperature test. The results of a temperature interrupted PFT test is shown in Figure 4(a). All the tests were performed to the same test load level.

The room temperature test primarily shows linear-elastic behavior. Following the room temperature result, the specimen is evaluated at  $600 \text{ }^\circ\text{C}$ . The increased compliance with temperature and the formation of a nearly-closed hysteresis loop at  $600 \text{ }^\circ\text{C}$  is related to the reduction of the misfit strain associated with thermal expansion anisotropy. This causes a relaxation of the clamping forces on bridging grains and lowers the bridging stress. Continuing to  $800 \text{ }^\circ\text{C}$ , it is observed that the deformation behavior then develops to a gross-slip condition.

Low cyclic loading tests were performed on a #5 PFT specimen, taken from about 7 mm behind the crack tip in a region of larger initial COD than the #1 PFT specimen. The #5 specimen therefore exhibits a lower stiffness and a lower peak load capacity than the #1 specimen<sup>24</sup>. Thus lower maximum load values were chosen for fatigue testing of this specimen. Figure 4(b) shows all of the test data obtained on the #5 PFT. As before, the material exhibits linear elastic behavior up to a maximum load of 0.15 Kg. The compliance also remains the same indicating that no fatigue degradation occurred up to this point in our test procedure.

However, by increasing the maximum load to 0.25 kg, we observe the formation of open loops indicating the predominant sliding mechanism activity discussed previously. We mention here the appearance of residual opening displacement that get larger as the load increases. It is also worth to mention that the stiffness of the loading and the unloading parts remain approximately the same, which means, from the contact point theory that even though sliding occurred during this set of tests (residual opening displacement), the distribution of contact point stays the same.

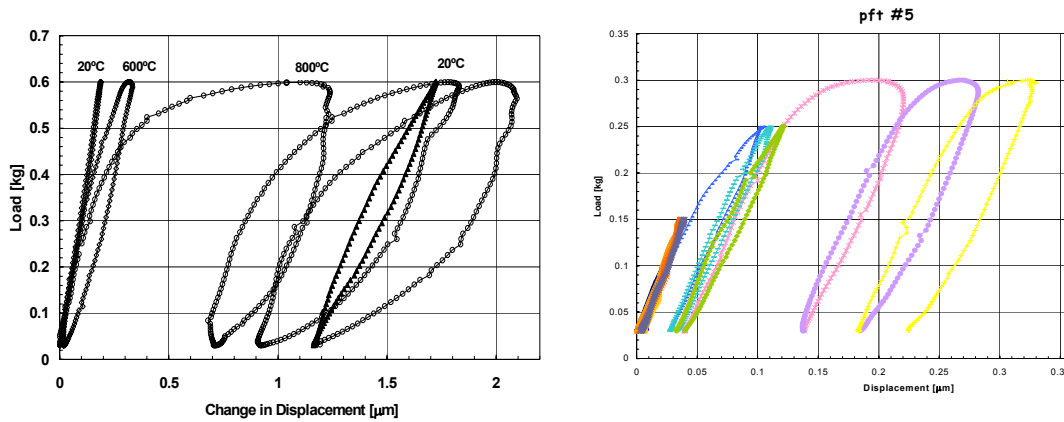


Figure 4: Effects of cyclic loading of PFT #5 (a) and of high temperature on PFT #2 (b)

## CONCLUSIONS

The post-fracture-tensile (PFT) technique has been successfully applied to an investigation of cyclic fatigue of wake zone processes in a commercial alumina at room and high temperature. At room temperature, when the peak loads and number of cycles were held below the critical values which cause frictional sliding of the grains, no fatigue damage was observed. Below these threshold points the material behaved linear elastically and no compliance changes were observed as a result of cycling. Above the threshold values, however, fatigue damage resulted from the fracture of the elastic ligaments and continuous sliding action of the grains. Also, the load at which non-linear behavior begins was seen to be reduced and the final loading compliance increased quite substantially. Final Results indicate that a frictional wear mechanism is activated after a certain number of cycles depending on the applied loads, allowing the bridging grains to slide in their sockets. This cumulative process reduces the effectiveness of the elastic

contact points of the wake mechanism as evidenced by the reduction in the length of the initial elastic region. Also, the frictional bridging stress was degraded which resulted in an increased compliance towards the end of the loading cycle. In PFT #5, situated far from the crack tip, it was clear from the results obtained that frictional sliding was the only bridging mechanism active, which is generally associated with residual crack opening displacements

Finally, the effects of temperature indicated some interesting properties of the TEA. Increasing the test temperature caused the reduction of the misfit strain associated with TEA. One can conclude that temperature increase caused the relaxation of the normal forces due to the softening behavior of the grain boundary phase. This effect was clear at 800 °C by the development of gross slip behavior or residual crack opening displacement.

*Acknowledgement-* Financial support for the initial formulation of this concept provided by USAFOSR Project #F49620-93-1-0210. All results and development of this approach were supported by DOE grant DE-FG03-96ER45577.

## REFERENCES

1. Evans, A. G., and Fuller, E. R., *Metall. Trans.*, 1974, **5** 27.
2. Krohn, D.A., Hasselman, D.P.H., *J. Am. Ceram. Soc.*, 1972, **55**(4), 208.
3. Guiu, F., *J. Mat. Sci. Lett.*, 1978, **13**, 1357.
4. Lathabai, S., Mai, Y-W., Lawn, B.R., *J. Am. Ceram. Soc.*, 1989, **72**(9), 1760.
5. Reece, M.J., Guiu, F., Sammur, M., *J. Am. Ceram. Soc.*, 1989, **72**(2), 348.
6. Kishimoto, H., Ueno, A., Okawara, S., *J. Am. Ceram. Soc.*, 1994, **77**(5), 1324.
7. Guiu, F., Li, M., Reece, M.J., *J. Am. Ceram. Soc.*, 1992, **75**(11), 2976.
8. Dauskardt, R.H., James, M.R., Porter, J.R., Ritchie, R.O., *J. Am. Ceram. Soc.*, 1992, **75**(4), 759.
9. Hu, Z-H, Mai, Y-W., *J. Am. Ceram. Soc.*, 1992, **75**(4), 848.
10. Dauskardt, R. H., *Acta Metall. Mater.*, 1993, **41**(9), 2765.
11. Gilbert, C. J., Petrany, R. N., Ritchie, R. O., Dauskardt, R. H. and Steinbrech, R. W., *J. Mater. Sci.*, 1995, **30**, 643.
12. Gilbert, C. J. and Ritchie, R. O., *Fatigue Fract. Engng. Mater. Struct.*, 1997, **20** [10] 1453.
13. Dauskardt, R. H., *Trans. of ASME – J. Eng. Mat. and Tech.*, 1993, **115** 244.
14. Jacobs, D.S., Chen, I-W., *J. Am. Ceram. Soc.*, 1995, **78**(3), 513.
15. Jacobs, D.S., Chen, I-W., *J. Am. Ceram. Soc.*, 1994, **77**(5), 1153.
16. Suresh, S., Han, L.X., Petrovic, J.J., *J. Am. Ceram. Soc.*, 1988, **71**(3), 158.
17. Gilbert, C. J., Dauskardt, R. H. and Ritchie, R. O., *J. Am. Ceram. Soc.*, 1995, **78**(9) 2291.
18. Buresch, F.E., Pabst, R., *Science Of Ceramics*, 1973, **6**(XVI), 3.
19. Steinbrech, R.W., Knehans, R., Schaarwachter, W., *J. Mater. Sci.*, 1983, **18**, 265.
20. Mai, Y.W., Lawn, B.R., *J. Am. Ceram. Soc.*, 1987, **70**(4), 289.
21. Swanson, P., Fairbanks, C.J., Lawn, B.R., Mai, Y.W., Hockey, B.J., *J. Am. Ceram. Soc.*, 1987, **70**(4), 279.
22. Vekinis, B., Ashby, M.G., Beaumont, P.W.R., *Acta metall. mater.*, 1990, **38**(6), 1151.
23. Lathabai, S., Rödel, J., Lawn, B.R., *J. Am. Ceram. Soc.*, 1991, **74**(6), 1340.
24. Hay, J.C., White, K.W., *J. Am. Ceram. Soc.*, 1995, **78**(4), 1025.
25. Hay, J.C., White, K.W., *Acta. Mater.*, 1997, **45**(9), 3625.
26. Hay, J.C., White, K.W., *J. Am. Ceram. Soc.*, 1997, **80**(5), 1293.
27. White, K.W., Hay, J.C., *J. Am. Ceram. Soc.*, 1994, **77**(9), 2283.
28. Steinbrech, R.W., Deuerler, F., Reichl, A., Schaarwachter, W., *Science of Ceramics*, 1988, **14**, 659.
29. Reichl, A., Steinbrech, R., *J. Am. Ceram. Soc.*, 1988, **71**(6), C299.
30. Hay, J.C., White, K.W., *J. Am. Ceram. Soc.*, 1993, **76**(7), 1849.